Author/s:
Priscilla, N;Li, N;Wesemann, L;Sulejman, S;Meng, J;Ako, RT;Bhaskaran, M;Sukhorukov, A;Roberts, A

Title:
High resolution bio-imaging via inverse design of metasurfaces

Date:
2024-03-08

Citation:
Priscilla, N., Li, N., Wesemann, L., Sulejman, S., Meng, J., Ako, R. T., Bhaskaran, M., Sukhorukov, A. & Roberts, A. (2024). High resolution bio-imaging via inverse design of metasurfaces. Razeghi, M (Ed.) Khodaparast, GA (Ed.) Vitiello, MS (Ed.) Proceedings Volume 12895, Quantum Sensing and Nano Electronics and Photonics XX, 12895, pp.70-70. SPIE. https://doi.org/10.1117/12.3000841.

Persistent Link:
https://hdl.handle.net/11343/345032

High Resolution bio-imaging via inverse design of metasurfaces

Niken Priscilla[a,d], Neuton Li[b,d], Lukas Wesemann[a,d], Shaban Sulejman[a,d], Jiajun Meng[a,d], Rajour Tanyi Ako[c,d], Madhu Bhaskaran[c,d], Andrey A. Sukhorukov[b,d], and Ann Roberts[a,d]

[a]School of Physics, The University of Melbourne, Parkville, Victoria, Australia
[b]Research School of Physics, Australian National University, Canberra, Australian Capital Territory, Australia
[c]Functional Materials and Microsystems Research Group, RMIT University, Melbourne, Victoria, Australia
[d]The Australian Research Council Centre of Excellence for Transformative Meta-Optical Systems (TMOS), Australia

ABSTRACT

Metasurfaces with angular sensitivity have been shown to provide a platform for developing an ultra-compact phase imaging system. Their performance, however, is often limited to a narrow range of spatial frequencies. Here, we apply inverse design to design and fabricate a metasurface an asymmetric optical transfer function across a numerical aperture (NA) of 0.6. The engineered response of this device enables phase imaging of microscopic transparent objects.

Keywords: Metasurface, Phase imaging, topological optimization, dielectric

1. INTRODUCTION

Image processing is commonly performed by first capturing an image with a digital camera and then manipulating it computationally. Because most conventional cameras are sensitive only to the amplitude of light, information such as phase is lost when the image is captured. Prior to the widespread availability of computational power, however, image processing operations were performed all optically and in real time by filtering spatial frequencies using a 4-f setup or similar configuration,[1] necessitating the use of bulky components and propagation distances. Unlike digital approaches, these methods permitted access to the phase of an optical field. Examples of these approaches include the Zernike phase contrast microscopy and the Differential Interference Contrast (DIC) microscopy. Metasurfaces offer an opportunity to develop a more compact alternative to optical components in translating phase gradient information into intensity with no digital post-processing. However, most existing meta-optical phase-imaging devices exhibit an optical transfer function with a near-linear dependence on spatial frequency over only a small range of spatial frequencies. This low NA of the devices results in image artifacts and reduced resolution for microscopic objects.[2] A crucial step forward in the field of meta-optical phase imaging devices is therefore the development of devices that perform well over a high numerical aperture.

We applied topological optimization via adjoint simulations[3] to design nontrivially shaped silicon nanoresonators on a sapphire substrate (Fig. 1 top middle). This dielectric device demonstrates an approximately linear and asymmetric OTF within a numerical aperture of 0.6 along the horizontal (x) direction. Due to the optical response of the device, phase information can be translated into intensity modulation which is correlated with the phase gradients. Our device enables visualization of phase objects such as unstained, live biological cells that otherwise present poor amplitude contrast and can only be weakly seen with a conventional camera. Its asymmetric response across a high NA has the potential to image biological cells of various sizes in high resolution.

Further author information: (Send correspondence to N.P.)
N.P.: E-mail: npriscilla@student.unimelb.edu.au
N.L.: E-mail: neuton.li@anu.edu.au

Quantum Sensing and Nano Electronics and Photonics XX, edited by Manijeh Razeghi, Giti A. Khodaparast, Miriam S. Vitiello, Proc. of SPIE Vol. 12895, 128950P
 · 0277-786X · doi: 10.1117/12.3000841

2. THEORY

Metasurfaces possess a unique capability of manipulating electric fields in a way that is not possible with traditional optics. In optical image processing, nonlocal metasurfaces with sensitivity to angles of incidence can be used to access and modify spatial frequency content of a wavefield directly in the object plane. Since the spatial frequency information can be altered at the object plane instead of the Fourier plane, the use of such metasurfaces allows a more compact image processing system. As monochromatic and spatially coherent light is incident on an imaging system, its wavefield can be decomposed into a superposition of plane waves traveling at various angles with respect to the optical axis. Taking the optical axis to be in the z-direction, the relationship between angles of incidences and transverse spatial frequency components is given by:

$$k_x = k_0 \sin\theta \cos\phi \tag{1}$$

$$k_y = k_0 \sin\theta \sin\phi \tag{2}$$

where $k_0 = 2\pi/\lambda$ for light of wavelength λ. The angle of propagation with respect to the optical axis is denoted by θ while ϕ is the angle between the projection of the wavevector to the $x-y$ plane and the $x-$ axis.

In Fourier space, the Fourier transform of the output image ($\vec{E}_{out}(k_x, k_y)$) from an optical system can be written as :

$$\vec{E}_{out}(k_x, k_y) = \vec{H}(k_x, k_y)\vec{E}_{in}(k_x, k_y) \tag{3}$$

where $\vec{E}_{in}(k_x, k_y)$ represents the incident wavefield and $\vec{H}(k_x, k_y)$ is a tensor that is referred to as the optical transfer function (OTF). The magnitude of the relevant component of this function is called the magnitude transfer function (MTF). One method to visualize phase information is to have a near linear MTF along one direction (e.g. $x-$ axis) while approximately constant in the orthogonal direction (e.g. $y-$ axis). This permits visualization of phase gradients along one direction similar to that seen in widely used differential interference contrast (DIC) microscopy. When this MTF operates on the spatial frequencies of a phase object, assuming the object contains spatial frequencies accessible to the MTF, features that are transparent to the traditional cameras can be observed with pseudo-3D contrast. To differentiate between positive and negative phase gradients without tilting the device, the MTF has to be asymmetric about $k_x = 0$.

The range of spatial frequencies where the transfer function remains approximately linear is referred to as the numerical aperture (NA) of the metasurface. This variable, in theory, imposes the spatial resolution of the features that can be observed through the metasurface ($\Delta x = \lambda/(2NA)$), but also depends on the properties of the entire imaging system.. Metasurfaces that have been shown to perform phase imaging at the object plane are commonly constrained to an NA of less than 0.2.[4–7] Here, we apply topological optimization to generate a unit cell design with a near-linear MTF up to an NA of 0.6.

3. NUMERICAL SIMULATION

To design the unit cells of the metasurface, we employ free-form topology optimization.[3] The device is optimized to have an asymmetrical optical transfer function over an NA of 0.6 along the $x-$ direction. The figure of merit is set to be the mean square error (MSE) between the current and the target transmitted amplitudes over a grid of spatial frequency points k_x/k_0, while the amplitude for orthogonal spatial frequencies (k_y/k_0) remained constant. Each step in the optimization process involves one forward and one adjoint simulation. The optical response of the device at each iteration is calculated via Rigorous Coupled Wave Analysis (RCWA) during forward simulation. The gradient of the figure of merit is calculated through a series of adjoint simulations. The iterations are performed until the figure of merit is minimized upon convergence. The optimization is performed for a unit cell of size 400 nm × 400 nm, such that higher order diffraction can be omitted at the observed spatial frequencies. Due to the symmetry of the design considered, the polarization of the incident light changes as it passes through the metasurface. Here, the input polarization is set to right circularly polarised (RCP) from the source point of view and observed through a left circularly polarised (LCP) analyzer. The operational wavelength of the device is chosen to be 750 nm.

The optimized unit cells consisting of silicon nanoresonators on sapphire are shown on top of Fig. 1 (top, center), while the two-dimensional MTF can be observed in Fig. 1 (center, lower). When an optical wavefield containing pure phase information, i.e., no amplitude variations, (Fig. 1 left) propagates through the device, the resulting image (top right) depicts a clear intensity image, highlighting phase gradients in the image, with few artifacts. This result is compared to an image produced by a device with an asymmetric transfer function across a constrained numerical aperture (NA $<$ 0.1) (Fig. 1 bottom right). It can be observed that the higher NA of the device contributes to improved resolution and a prominent reduction in artifacts. Our device potentially provides an alternative to a compact all-optical image processing in the realm of high-resolution phase imaging.

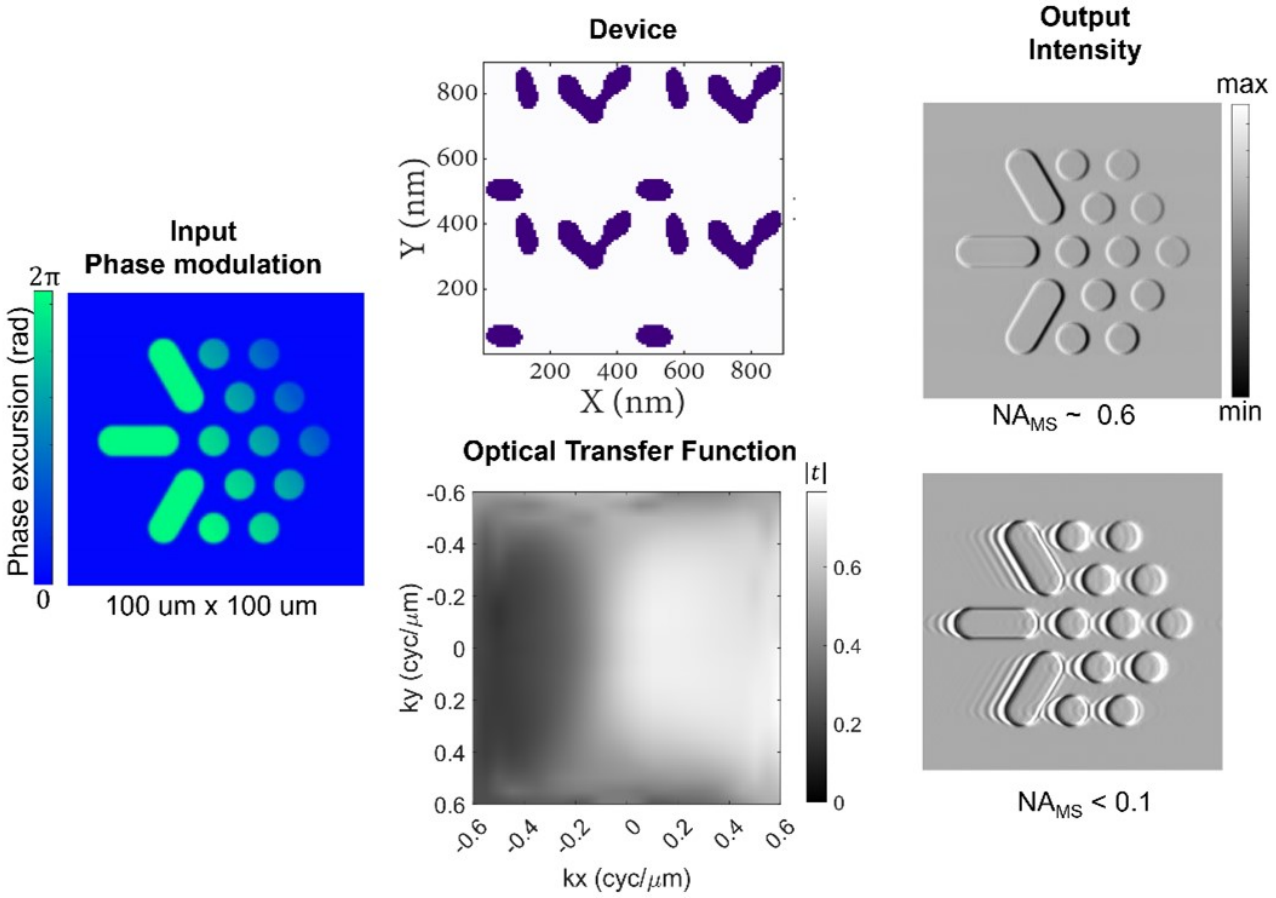

Figure 1. Numerical simulation of image processing through the metasurface. (left) Phase modulation input is invisible to the standard camera. (middle top) A binary schematic of the 2 x 2 unit cells of the device showing silicon nanoresonators on a sapphire substrate and (middle bottom) its respective 2-D Optical Transfer Function. (right-top) Optically processed intensity image resulting from the propagation of phase modulation input (left) through the device (middle). The resolution of the image increased significantly ($NA_{MS} \approx 0.6$) compared to the intensity output (right bottom) through a metasurface with a linear transfer function across a narrow spatial frequency range ($NA_{MS} < 0.1$).[6]

4. EXPERIMENTAL RESULTS

The fabrication of the device involves a standard electron beam lithography technique. One-micron crystalline silicon on a sapphire substrate is coated with a 200 nm thick layer of PMMA which functions as a positive resist. Then electron beam lithography is performed, where the beam is exposed to designated areas where the PMMA is dissolved during the development process. Then, a 30 nm thick layer of alumina is evaporated onto the substrate, followed by a lift-off process. The pattern covered by alumina acts as a mask during the etching

process (Fig. 2 b). Reactive ion etching was performed to etch down 1 micron of silicon on the areas where the alumina mask is absent. A scanning electron microscopy photograph of the completed device is shown in (Fig. 2 c).

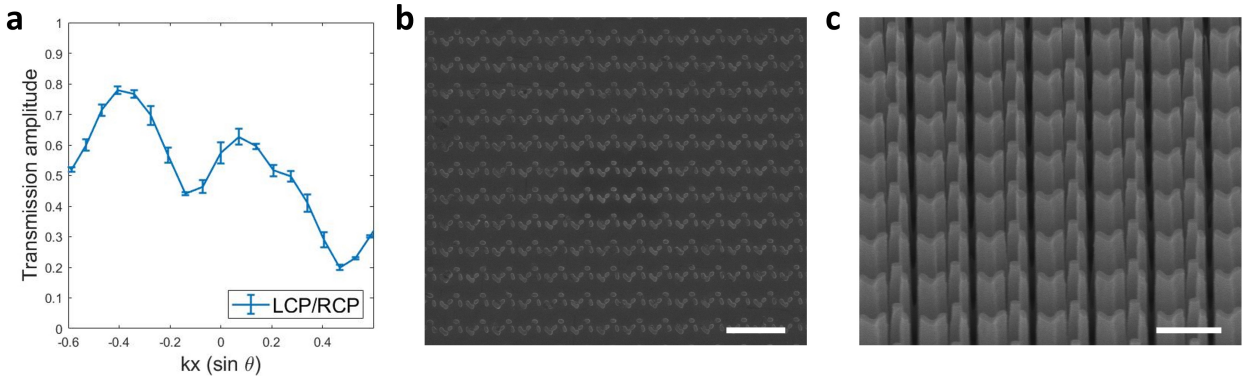

Figure 2. (a) Experimental measurement of the device magnitude transfer function (MTF) shows an asymmetric trend across an NA of ≈ 0.6 in the cross-polarized component at the operational wavelength of 758 nm. Scanning electron microscopy photographs of the device (b) before the etching process (scale bar is 1 μm) and (c) after the etching process (scale bar is 500 nm).

The modulation transfer function of the device is measured via a transmission setup. The sample is illuminated by filtered white light that has been passed through a linear (horizontal) polarizer and a quarter waveplate that is oriented at 45° to the polarizer. The transmission through the sample is analyzed with another linear (vertical) polarizer and a quarter waveplate oriented at 45° to the vertical polarizer, to capture the cross-polarised components. The transmission response of the sample is captured as the sample is tilted from $-40°$ to 40° in steps of 4°. Transmission is normalized to the incident power and the square root of the intensity obtained is used to calculate the transmission amplitude. The MTF of the device (Fig. 2 a) at 758 nm $\pm$ 3 nm shows an asymmetric trend, indicating about 60 % contrast across an NA of almost 0.6. The incident polarization here is set to LCP when viewed from the source and the analyzer to RCP. While there is a strong deviation from the linear trend in the experimental data, The asymmetric trend in the transfer function can be used to image phase objects. We believe that further improvements can be made in terms of better convergence in the optimization process to ensure a linear function. Due to the nontrivial shapes of the resonators, however, imperfections in the fabrication process may also contribute to the deviation.

We demonstrate the capability of our device to visualize phase modulations with weak amplitude contrast. The first phase object is a checkered pattern (Fig. 3 b) generated with a spatial light modulator (SLM). The variations in phase are not visible when directly imaged by the camera (Fig. 3 a left). When the metasurface is placed in front of the SLM projection, however, the checkered patterns appear with some of the edges being highlighted (Fig. 3 a right). This highlight and the placement of the shadows create pseudo-3D features that are reminiscent of differential interference microscopy (DIC), which is a conventional phase imaging method. Yeast cells were also placed in the imaging system. Without the presence of the metasurface (Fig. 3 d), the cells have insufficient contrast when imaged through the camera. When the metasurface is placed against the same area, individual cells on the glass slides can be distinguished (Fig. 3 d). In the areas marked by the red circles, it can be observed that the samples are more clearly visible when the metasurface is present.

5. CONCLUSION

We have shown a compact method for phase imaging via a dielectric metasurface across a numerical aperture of 0.6. This device has the potential to eliminate the need for bulk optics for high resolution phase imaging. We anticipate that the method of inverse design to image processing meta-optics can be applied to generate devices with a variety of optical transfer functions with the possibility of integrating multiple responses in one device.

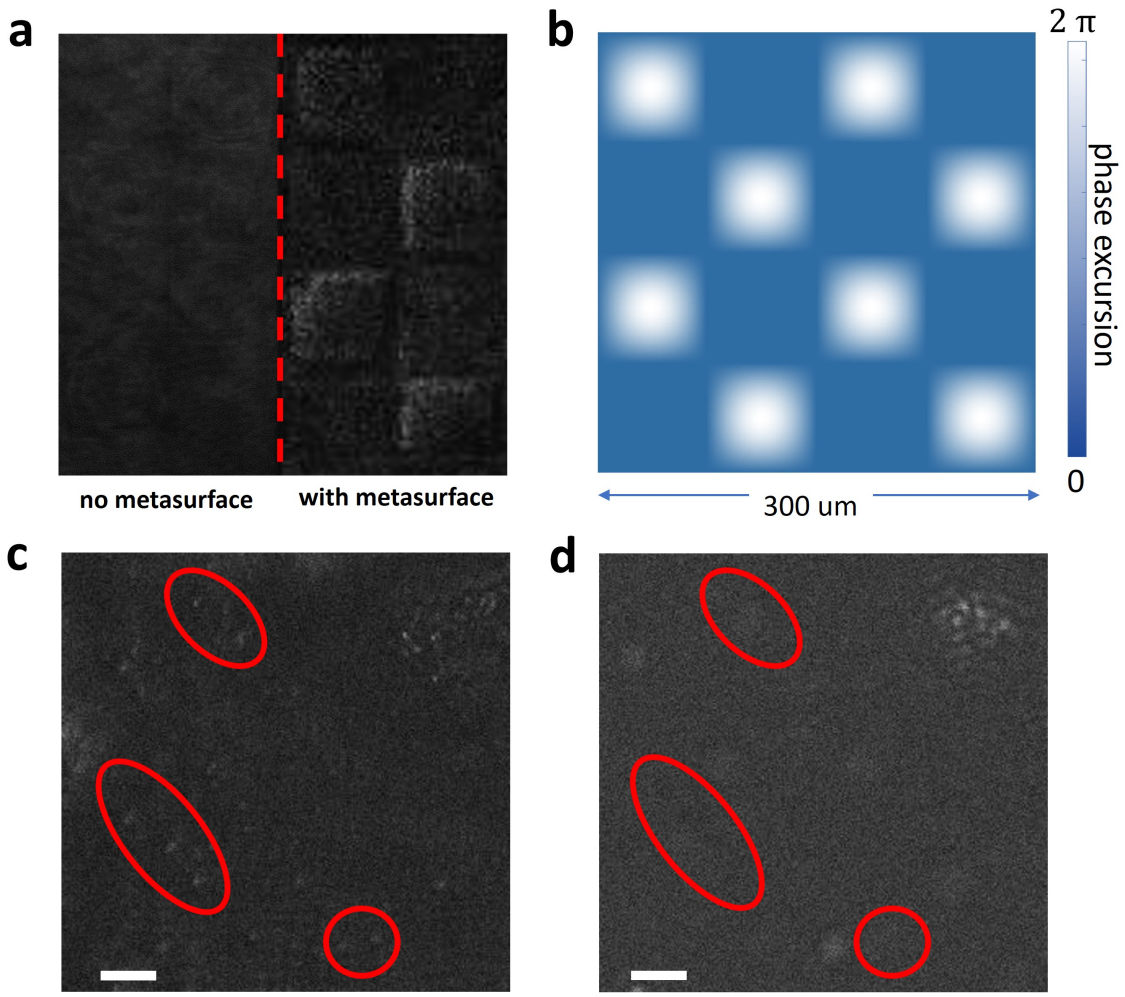

Figure 3. Observations of phase objects through the metasurface. (a) A spatial light modulator (SLM) was used to project a phase object of a checkered board pattern to the metasurface. The checkered pattern is only visible when the metasurface is placed in the imaging system. (b) The phase modulation projected by the SLM in (a). (c) Yeast cells placed against the metasurface at the object plane. The cells are only visible in the presence of the metasurface. (d) Yeast cells as observed with a coherent light source without the presence of metasurface. (c), (d) red circles mark the same viewing areas, scale bars are 30 μm.

Further development in this field will be advantageous for quantitative phase imaging and can reduce the amount of computational post-processing required for image manipulation.

ACKNOWLEDGMENTS

This research was conducted by the Australian Research Council Centre of Excellence/ARC Special Research Centre/ARC Key Centre for Transformative Meta-Optical Systems (project number CE200100010) and funded by the Australian Government. This work was performed in part at the Melbourne Centre for Nanofabrication (MCN) in the Victorian Node of the Australian National Fabrication Facility (ANFF).

REFERENCES

[1] Goodman, J. W., [*Introduction to Fourier optics / Joseph W. Goodman.*], Roberts Co., Englewood, Colo, 3rd ed. ed. (2005).

[2] Wesemann, L., Davis, T. J., and Roberts, A., "Meta-optical and thin film devices for all-optical information processing," *Applied Physics Reviews* **8**, 031309 (08 2021).

[3] Molesky, S., Lin, Z., Piggott, A. Y., Jin, W., Vucković, J., and Rodriguez, A. W., "Inverse design in nanophotonics," *Nature Photonics* **12**, 659–670 (Nov 2018).

[4] Wesemann, L., Rickett, J., Song, J., Lou, J., Hinde, E., Davis, T. J., and Roberts, A., "Nanophotonics enhanced coverslip for phase imaging in biology," *Light: Science & Applications* **10**, 98 (May 2021).

[5] Zhang, X., Zhou, Y., Zheng, H., Linares, A. E., Ugwu, F. C., Li, D., Sun, H.-B., Bai, B., and Valentine, J. G., "Reconfigurable metasurface for image processing," *Nano Letters* **21**(20), 8715–8722 (2021). PMID: 34643401.

[6] Wesemann, L., Rickett, J., Davis, T. J., and Roberts, A., "Real-time phase imaging with an asymmetric transfer function metasurface," *ACS Photonics* **9**(5), 1803–1807 (2022).

[7] Ji, A., Song, J.-H., Li, Q., Xu, F., Tsai, C.-T., Tiberio, R. C., Cui, B., Lalanne, P., Kik, P. G., Miller, D. A. B., and Brongersma, M. L., "Quantitative phase contrast imaging with a nonlocal angle-selective metasurface," *Nature Communications* **13**, 7848 (Dec 2022).